J. Space Weather Space Clim. 2023, **13**, 28

https://doi.org/10.1051/swsc/2023027

JSWSC

Available online at:
www.swsc-journal.org

TECHNICAL ARTICLE OPEN ACCESS

On the detection of a solar radio burst event that occurred on 28 August 2022 and its effect on GNSS signals as observed by ionospheric scintillation monitors distributed over the American sector

Isaac G. Wright[1], Fabiano S. Rodrigues[1,*], Josemaria Gomez Socola[1], Alison O. Moraes[2], João F. G. Monico[3], Jan Sojka[4], Ludger Scherliess[4], Dan Layne[5], Igo Paulino[6], Ricardo A. Buriti[6], Christiano G. M. Brum[7], Pedrina Terra[7], Kshitija Deshpande[8], Pralay R. Vaggu[8], Philip J. Erickson[9], Nathaniel A. Frissell[10], Jonathan J. Makela[11], and Danny Scipión[12]

[1] The University of Texas at Dallas, Richardson, TX 75080, USA
[2] Institute of Aeronautics and Space, São José dos Campos, SP 12228, Brazil
[3] Universidade Estadual Paulista – UNESP, Presidente Prudente, SP 13506, Brazil
[4] Utah State University, Logan, UT 84322, USA
[5] Deep Space Exploration Society, Colorado Springs, CO 80918, USA
[6] Federal University of Campina Grande, Campina Grande, PB 58429, Brazil
[7] Florida Space Institute, University of Central Florida, Orlando, FL 32826, USA
[8] Embry-Riddle Aeronautical University, Daytona Beach, FL 32114, USA
[9] MIT Haystack Observatory, Westford, MA 01886, USA
[10] The University of Scranton, Scranton, PA 18510, USA
[11] University of Illinois Urbana-Champaign, Urbana, IL 61801, USA
[12] Instituto Geofisico del Peru, Radio Observatorio de Jicamarca, Lima 15012, Peru

Received 25 July 2023 / Accepted 19 October 2023

Abstract – As part of an effort to observe and study ionospheric disturbances and their effects on radio signals used by Global Navigation Satellite Systems (GNSS), alternative low-cost GNSS-based ionospheric scintillation and total electron content (TEC) monitors have been deployed over the American sector. During an inspection of the observations made on 28 August 2022, we found increases in the amplitude scintillation index (S_4) reported by the monitors for the period between approximately 17:45 UT and 18:20 UT. The distributed, dual-frequency observations made by the sensors allowed us to determine that the increases in S_4 were not caused by ionospheric irregularities. Instead, they resulted from Carrier-to-Noise (C/No) variations caused by a solar radio burst (SRB) event that followed the occurrence of two M-class X-ray solar flares and a Halo coronal mass ejection. The measurements also allowed us to quantify the impact of the SRB on GNSS signals. The observations show that the SRB caused maximum C/No fadings of about 8 dB-Hz (12 dB-Hz) on L1 ~ 1.6 GHz (L2 ~ 1.2 GHz) for signals observed by the monitor in Dallas for which the solar zenith angle was minimum (~24.4°) during the SRB. Calculations using observations made by the distributed monitors also show excellent agreement for estimates of the maximum (vertical equivalent) C/No fadings in both L1 and L2. The calculations show maximum fadings of 9 dB-Hz for L1 and of 13 dB-Hz for L2. Finally, the results exemplify the usefulness of low-cost monitors for studies beyond those associated with ionospheric irregularities and scintillation.

Keywords: Solar radio burst / SRB / GPS / GNSS / fading / space weather

*Corresponding author: fabiano@utdallas.edu

1 Introduction

It is well-recognized that space weather events can impact technological systems, particularly those that rely on trans-ionospheric radio systems (e.g., Coster et al., 2021). For instance, irregularities in the ionospheric plasma density are an important component of space weather. Ionospheric irregularities cause the diffraction of radio waves resulting in rapid variations in the amplitude and/or phase of trans-ionospheric radio signals received on the ground or in space (Yeh & Liu, 1982). Ionospheric irregularities and scintillation represent major threats to the performance of various civilian and military systems (e.g., Ishimaru et al., 1999; Kintner et al., 2007; Kelly et al., 2014). To advance our capability to monitor and study ionospheric irregularities and scintillation, Gomez Socola & Rodrigues (2022) developed low-cost GNSS-based ionospheric total electron content (TEC) and scintillation monitors. While these monitors are not intended to fully replace commercial monitors, they are a cost-effective alternative for a variety of studies. For instance, Sousasantos et al. (2023) used observations made by these monitors to detect and study an event of extreme plasma bubbles (EPBs) reaching mid-latitudes. Recently, a number of these sensors started to be deployed over the American sector for studies of low and mid-latitude ionospheric irregularities and L-band scintillation.

Space weather phenomena are ultimately driven by solar activity. For instance, a solar flare is a sudden and intense burst of electromagnetic radiation emitted by the Sun, which can last from minutes to hours. It is caused by the release of magnetic energy stored in the solar atmosphere, often in regions of intense magnetic fields called active regions or sunspots (Bastian et al., 1998). Another noteworthy solar event is a Coronal Mass Ejection (CME) which can be described as a sudden and large expulsion of magnetized plasma from the sun. Often, events referred to as Solar Radio Bursts (SRBs) are observed accompanying solar flares and CMEs. SRBs can be described as brief periods when solar emissions in the radio frequency band are elevated with respect to typical background levels. SRBs are known to occur over a wide band of frequencies. The primary mechanism responsible for SRBs that occur around the L-band region is thought to be plasma radiation. During a solar flare, for instance, electrons are accelerated from the active region by magnetic reconnection. The acceleration of the electron beam through the ambient plasma creates instabilities in the solar plasma that give rise to plasma waves. These plasma waves can be converted into electromagnetic waves with frequency related to the electron plasma frequency. These electromagnetic waves comprise the SRB (Bastian et al., 1998). In addition to magnetic reconnection, it has been pointed out that a sufficiently fast and wide CME could generate a plasma shock by which particles are driven to high enough energies to excite the plasma waves responsible for SRBs (e.g., Claßen & Aurass, 2002; Morosan et al., 2021).

If an SRB occurs with significant emission in the L-band region (1–2 GHz) and with Right-Hand Circular Polarization (RHCP), it could affect the signals and the performance of global navigation satellite systems (GNSS). This would occur as a result of an increase in the background noise levels and, consequently, a decrease in the Carrier-to-Noise Ratio (C/No) of the GNSS signals (Klobuchar et al., 1999). For instance, Cerruti et al. (2008) reported the impact of an SRB associated with the X6.5 solar flare of December 6, 2006. The SRB exceeded 1,000,000 Solar Flux Units (SFU) at the L1 frequency and caused fadings in GPS L1 signals of up to 25 dB. GPS receivers that are part of the International GNSS Service (IGS) Network experienced decreases in the number of tracked signals during the SRB. Further analyses by Carrano et al. (2009) showed peak positioning errors in the horizontal and vertical directions of 20 m and 60 m, respectively, for GNSS receivers during this SRB event.

The occurrence rate of ionospheric irregularities leading to L-band scintillation is fairly common, particularly at low latitudes during Equinoxes and December solstice, and has been reported extensively (e.g., Basu et al., 1980; Groves et al., 1997; de Paula et al., 2003; Valladares et al., 2004; Kintner et al., 2007; Muella et al., 2010; Moraes et al., 2012; Spogli et al., 2013; Jiao & Morton, 2015; Correia et al., 2019). SRBs, however, do not occur as frequently and a limited number of studies describing their effects on GNSS signals have been reported. For instance, in 2018, Yue et al. (2018) reported that only eight SRBs events and their effects on GNSS had been reported. A review of the literature for this study identified the following studies describing the impact of SRBs on GNSS signals: Chen et al. (2005), Cerruti et al. (2006, 2008), Afraimovich et al. (2008, 2009); Carrano et al. (2009); Demyanov et al. (2012), Yue et al. (2013), Sreeja et al. (2013, 2014), Muhammad et al. (2015), Sato et al. (2019), and de Paula et al. (2022).

Here we contribute by reporting the observations of a new L-band fading event associated with an SRB observed on 28 August 2022. The event was detected by a network of GNSS-based scintillation and TEC monitors (ScintPi 2.0 and 3.0) distributed over the United States and South America. We point out that the Owens Valley Solar Array (OVSA) has observed SRBs and has provided important information about these events for the American longitude sector (e.g., Nita et al., 2004). On 28 August 2022, however, the current version of OVSA (Expanded OSVA – EOVSA) was not operating during this event. Therefore, in addition to reporting and quantifying the effects of a new SRB on GNSS signals, the observations also contribute to L-band solar observations in the American sector.

The report is organized as follows: In Section 2, we describe the instrumentation used in this study. We provide information about the measurements available and the location of the instrumentation. In Section 3, we present and discuss the observations and main results. The discussion includes comparisons with auxiliary satellite measurements and quantification of the SRB effects. Finally, in Section 4, we summarize our main findings.

2 Instrumentation

The measurements used in this study were made by ScintPi 2.0 and 3.0 monitors. ScintPi 3.0 can be described as a low-cost GNSS-based ionospheric scintillation and TEC monitor. It can measure amplitude scintillation on L1 ~ 1.6 GHz and L2 ~ 1.2 GHz signals transmitted by the following GNSS constellations: GPS, Galileo, GLONASS, Beidou, and SBAS. ScintPi 3.0 can also measure ionospheric TEC. ScintPi 2.0 is a lower-cost monitor that can only measure amplitude scintillation on L1 signals transmitted by GPS, Galileo, GLONASS, Beidou, and SBAS. The reduced cost of these monitors is due to lower sampling rate (10–25 Hz) and resolution

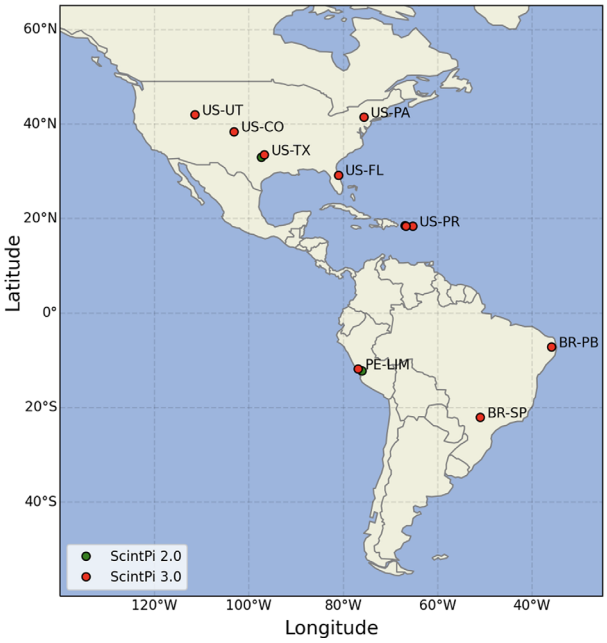

Monitor	Location	Latitude	Longitude
ScintPi 2.0	Jicamarca, PE-LIM	11.95° S	76.88° W
ScintPi 2.0	Texas, US-TX	32.99° N	96.76° W
ScintPi 3.0	Jicamarca, PE-LIM	11.95° S	76.88° W
ScintPi 3.0	Texas, US-TX	32.99° N	96.76° W
ScintPi 3.0	Florida, US-FL	29.19° N	81.05° W
ScintPi 3.0	Pennsylvania, US-PA	41.41° N	76.66° W
ScintPi 3.0	Colorado, US-CO	38.38° N	103.16° W
ScintPi 3.0	Utah, US-UT	41.93° N	111.42° W
ScintPi 3.0	Quebradillas, US-PR	18.47° N	66.91° W
ScintPi 3.0	Culebra, US-PR	18.33° N	65.31° W
ScintPi 3.0	Arecibo, US-PR	18.35° N	66.75° W
ScintPi 3.0	Paraiba, BR-PB	7.213° S	35.907° W
ScintPi 3.0	Pres. Prudente, BR-SP	22.12° S	51.41° W

Figure 1. Map with the location of the ScintPi monitors that were collecting data on 28 August 2022. The geographic coordinates of the monitors used in this study are also shown on the right.

of C/No (1 dB-Hz) measurements compared to commercial receivers. Gomez Socola & Rodrigues (2022) provide a comprehensive description of ScintPi 2.0 and 3.0. Additionally, Rodrigues & Moraes (2019) and Gomez Socola & Rodrigues (2022) show that, despite the lower sampling rate and resolution, low-cost monitors can provide excellent estimates of scintillation severity compared with commercial counterparts.

Scintillation activity is determined by ScintPi 2.0 and 3.0 using high-rate measurements of signal amplitude. Scintillation activity is quantified by the traditional S_4 index, which can be described as the standard deviation of signal amplitude normalized by its average (Yeh & Liu, 1982):

$$S_4 = \sqrt{\frac{\langle I^2 \rangle - \langle I \rangle^2}{\langle I \rangle^2}}, \quad (1)$$

where I represent the amplitude of the GNSS signal, and the angle brackets represent the ensemble average. Signal amplitude values come from linearized values of C/No provided by GNSS receivers. In practice, averages are calculated in 1-minute intervals. ScintPi monitors and quantifies amplitude scintillation using the S_4 index. For this study, we utilize products produced by the ScintPi receivers which include L1 and L2 S_4 indices, TEC, and L1 and L2 C/No values.

Figure 1 shows the locations of the ScintPi 2.0 and 3.0 distributed over the American sector whose measurements were available for this study. The monitors are hosted by universities, observatories, and citizen scientists.

3 Results and discussions

On 28 August 2022, the ScintPi 3.0 monitor deployed in Dallas, US detected a clear increase in the magnitude of the S_4 values. Panels (a1) and (a2) in Figure 2 show the L1 and L2 S_4 values, respectively, observed on 28 August 2022. The panels show S_4 values for all satellites with elevation greater than 25°. More importantly, they show that the S_4 indices reached values as high as 0.5 in both frequencies around 18:00 UT.

L-band scintillation at mid-latitudes is a rare event with limited observations reported in the literature (e.g., Mrak et al., 2020; Rodrigues et al., 2021; Ledvina et al., 2002). Additionally, the observations show a few unusual features. For instance, increases in the S_4 value were found to occur simultaneously in all signals tracked at the time. Additionally, the increase in S_4 occurred during daytime hours when ionospheric F-region irregularities were not expected to find favorable growth conditions.

Further inspection of the C/No measurements also shows unusual long-lasting deep fadings. This is illustrated in L1 and L2 measurements for GPS SVID 15 on 28 August 2022 shown in panels (b1) and (b2) of Figure 2, respectively. GPS SVID 15 was selected to be shown here because it illustrates well the increases in S_4 and fadings observed on this day and because the signals from this satellite are observed by most monitors in the network. To better illustrate the depth of the fadings, we also show the C/No for the previous day, 27 August. It can be seen that the C/No for the L1 signal dropped to about 40 dB-Hz and that the C/No for L2 dropped to less than 35 dB-Hz during the time when the S_4 increases were observed.

Additionally, we found that the fadings were not accompanied by perturbations in TEC which confirm that increases in S_4 were not associated with ionospheric irregularities. This is illustrated in Figure 2c. It shows, the relative ionospheric TEC derived from differential phase measurements for GPS SVID 15. The smooth TEC curve does not show any indication of irregularities during the fading event.

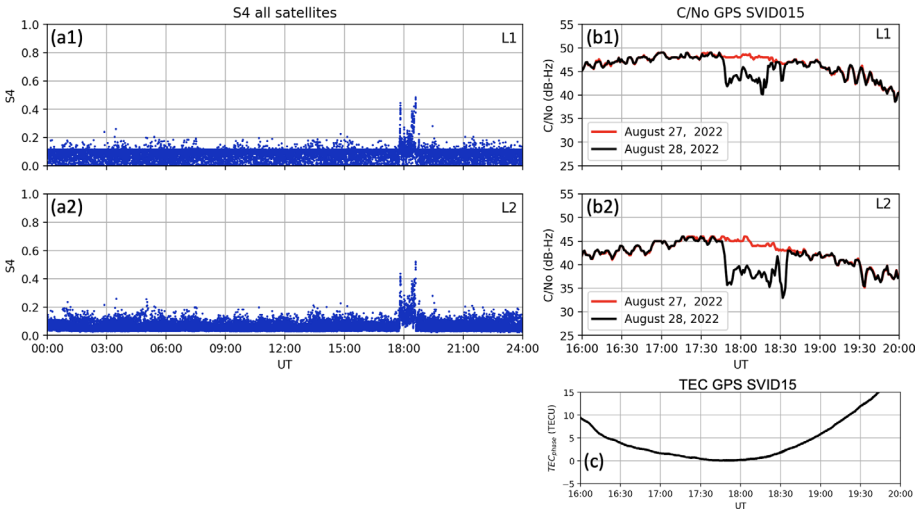

Figure 2. S_4 values observed in the L1 (a1) and L2 signals (a2) transmitted by GPS SVID 15 and observed by the Dallas ScintPi 3.0 monitor. S_4 for signals from all satellites with elevation greater than 25° are shown. C/No values for L1 (b1) and L2 signals (b2) transmitted by GPS SVID 15. Panel (c) shows the TEC estimated from L1 and L2 phase measurements for GPS SVID 15.

3.1 On the solar activity and associated SRB of 28 August 2022

The features in the observations made by the ScintPi monitor in Dallas led us to consider a solar event as the source of the fadings. We found that, indeed, strong solar activity was observed around the occurrence of the fadings. They were related to Active Region 3088 (AR3088) which was associated with several solar flares and CMEs.

In particular, we noted that two M-Class solar flares occurred around the time of the fadings on 28 August 2022. The National Oceanic and Atmospheric Administration (NOAA) reported an M6.7 class solar flare that started at 15:48 UT, lasted until 16:46 UT, and peaked at 16:19 UT. After that, a less intense M4.6 flare was reported lasting from 18:20 UT to 18:50 UT, with a peak at 18:32 UT. Figure 3 shows solar X-ray flux measurements made by the GOES 17 satellite on two bands, 0.1–0.8 nm (black curve) and 0.05–0.4 nm (red curve) between 27 and 29 August 2022. It illustrates the high occurrence of solar flares associated with AR3088. In addition to X-ray solar flares, we also point out the occurrence of a Halo CME reported by the Large Angle and Spectrometric Coronagraph (LASCO) at 16:12 UT on 28 August and has a linear speed of 1232 km/s.

During this period of intense solar activity, NOAA also reported the occurrence of a SRB measuring 230,000 SFU at 1415 MHz (1 SFU = 10^{-22} $Wm^{-2}Hz^{-1}$). The event was detected by the Radio Solar Telescope Network (RSTN) station at Palahua, US. The event occurred between 17:13 UT and 19:59 UT with a peak at 18:30 UT.

Estimates of the lower bound of the strength of an SRB required to affect L1 GNSS signals vary from 40,000 SFU (Klobuchar et al., 1999) to 10,000 SFU (Demyanov et al., 2012). Therefore, the SRB of magnitude of 230,000 SFU as reported by NOAA on 28 August 2022 is well above the theoretical thresholds for an observable effect. More importantly, the time during which the SRB was observed (17:13 UT to 19:59 UT) coincides well with the occurrence of the observed increased S_4 and fadings (~17:45 to 18:30 UT). In addition to solar X-ray measurements, previous studies of GNSS signal fadings observed over the US correlated these events with radio observations provided by the Owens Valley Solar Array (OVSA) (Carrano et al., 2009; Cerruti et al., 2006, 2008). Unfortunately, OVSA was not making observations on 28 August 2022. But this highlights how GNSS-based monitors such as ScintPi can contribute to SRB monitoring and space weather studies.

3.2 On the distributed GNSS-based observations

Having access to distributed observations (see Fig. 1) made by similar instruments allowed us to investigate the spatial extent of the impact of the SRB on GNSS signals.

Panels (a1)–(a13) in Figures 4 show the S_4 L1 observations made on 28 August 2022 by the 13 monitors located at the 11 sites used in this study (see Fig. 1). Again, an elevation mask of 25° was applied to minimize multipath artifacts. The background S_4 values for each sensor can be explained by differences in the installations. Nonetheless, the receivers in the network experienced a concurrent enhancement in S_4 values. A closer inspection of the data shows that enhancement occurred between 17:45 UT and 18:30 UT like what had been observed in Dallas.

To better evaluate the impact of the SRB on GNSS signals, we also inspected the C/No values measured by all the sensors listed in the table shown in Figure 1. Panels (b1)–(b13) in Figure 4 show the L1 C/No signals measured by the stations on 28 August 2022 for an elevation mask of 25°. The observations show a similar C/No fading pattern in the L1 signals observed by all the receivers. Again, the fading occurs simultaneously in all receivers between approximately 17:45 UT and 18:30 UT just like what had been observed by the Dallas receivers. A closer inspection of the observations, however, shows that the maximum fading depth varied from receiver to receiver. This variation in fading depth is examined next.

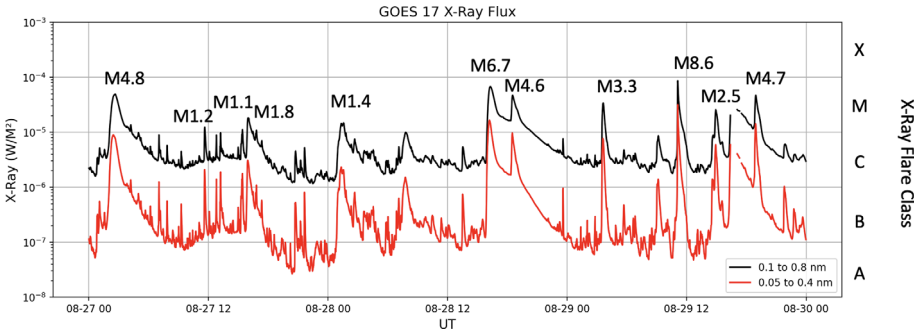

Figure 3. Solar X-ray flux measured by the GOES 17 Solar X-ray Imager on between 27 to 29 August 2022 for wavelengths 0.1–0.8 nm (black) and 0.05–0.4 nm (red). Two M-class events were observed around the time of the reported SRB (~18:30 UT).

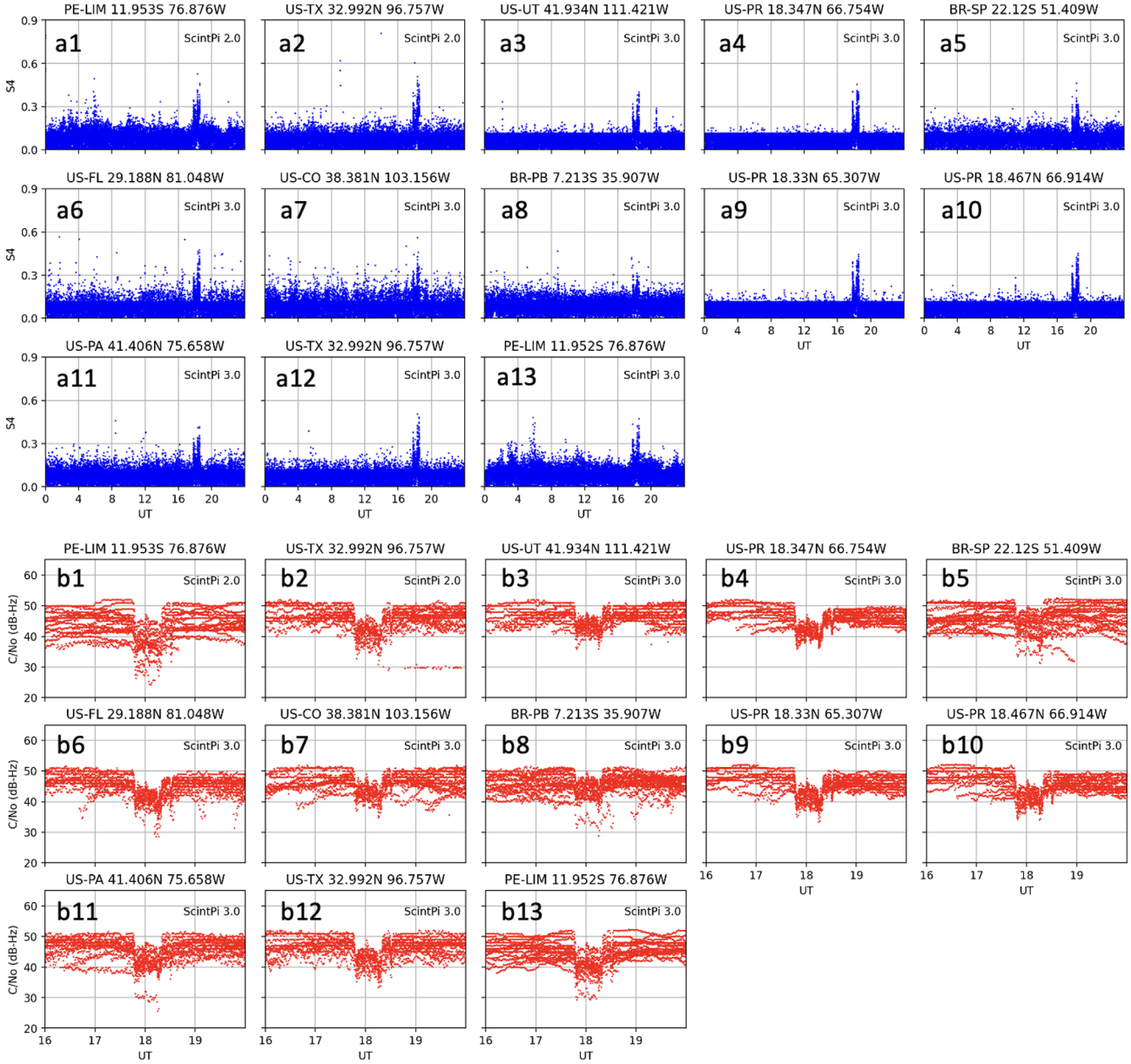

Figure 4. (a1)–(a13) L1 S_4 measured by the ScintPi monitors on 28 August 2022. The increase in S_4 values between about 17:30 UT and 18:15 UT and associated with the SRB can be observed in the data from all the receivers. (b1)–(b13) L1 C/No measured by the ScintPi on 28 August 2022. The observations show a similar C/No fading pattern in all L1 signals observed by the receivers.

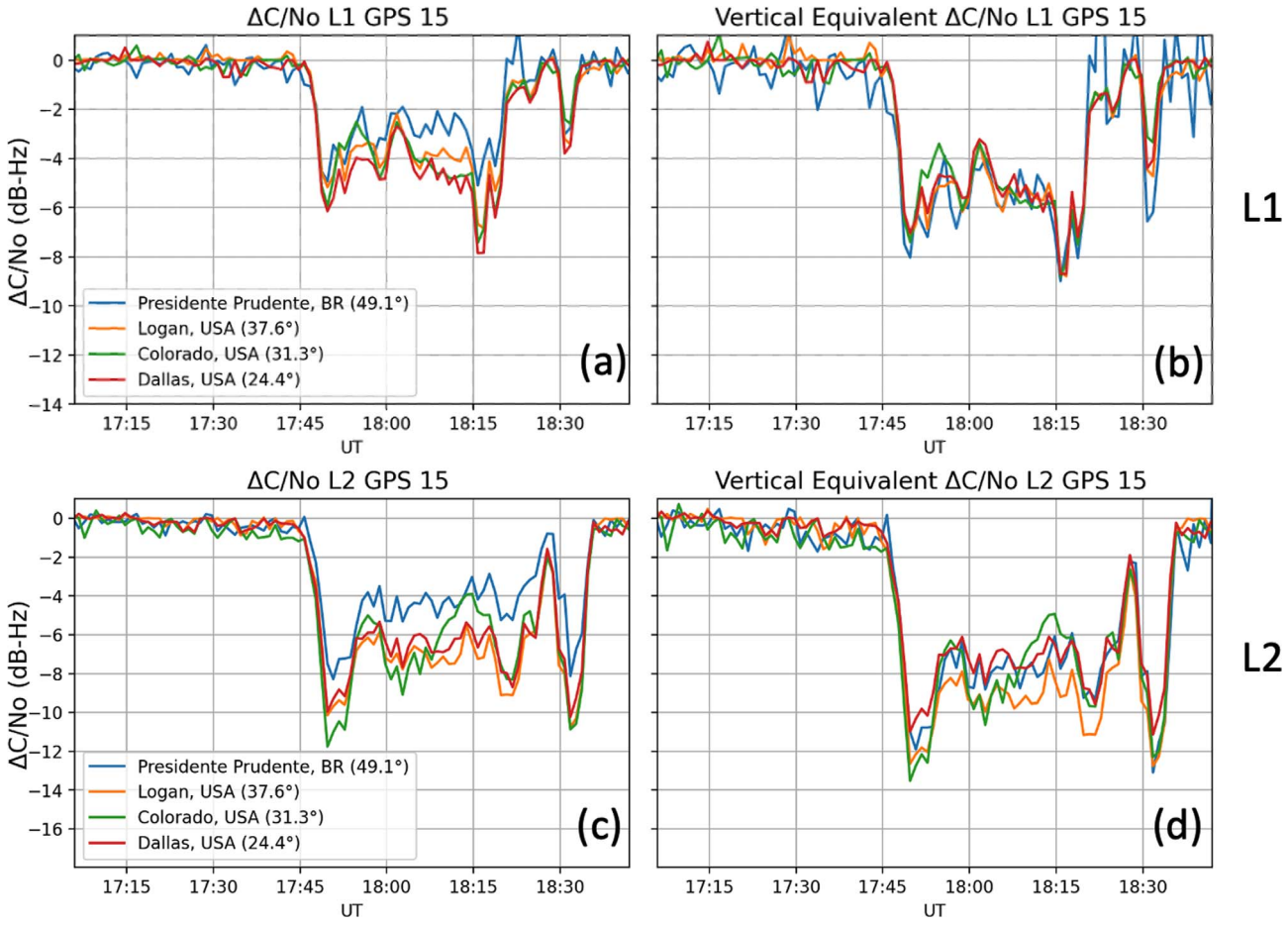

Figure 5. (a) L1 ΔC/No for observations made on 28 August 2022 by monitors located at different sites. The solar zenith angle at 18:00 UT is indicated for each site. (b) Vertical equivalent L1 ΔC/No fadings for the same stations. (c) L2 ΔC/No for observations made on 28 August 2022 by monitors located at different sites. The solar zenith angle at 18:00 UT is indicated for each site. (d) Vertical equivalent L2 ΔC/No fadings for the same stations.

3.3 On estimates of maximum, zenith equivalent, SRB fadings

The distributed ScintPi sensors provide us with measurements of the impact of the 28 August 2022 SRB on GNSS signals for receivers under different solar zenith angle conditions. We now examine the agreement between the distributed observations by estimating the maximum, solar zenith equivalent, C/No fading that could have been caused by the 28 August 2022 SRB.

Carrano et al. (2009) pointed out that the maximum fading caused by an SRB can be estimated by taking into consideration the solar zenith angle (θ) and the gain pattern of the GNSS antenna, represented by a function $g(\theta)$. More specifically, they derived an expression for the vertical (zenith) equivalent, $(C/No)^Z(\theta)$, that would have been measured if the GNSS receiver were located at the sub-solar point ($\theta = 0°$). The expression is given by:

$$(C/No)^Z(\theta) = (C/No)^0 \left\{ 1 + \frac{g(0)}{g(\theta)} \left[\frac{(C/No)^0}{(C/No)} - 1 \right] \right\}^{-1}, \quad (2)$$

where $(C/No)^0$ represents the C/No that would have been observed by a receiver without the effects of an SRB. For our analyses here, we focus on measurements made using the GPS SVID 15 signals. In addition to this signal being observed by multiple monitors, the orbit of GPS satellites allows us to use measurements from the previous day as an estimate of $(C/No)^0$. The ratio $(C/No)^0/(C/No)$ represents the C/No fade due to the SRB, in linear units. The terms $g(\theta)$ and $g(0)$ represent the gain of the antenna at angles θ and 0, respectively. Similar to Carrano et al. (2009), we estimated $g(\theta)$ using a Gaussian function fitted to gain values provided by the manufacturer of the antenna (Abracon model AEAGMK148060-S1575). Estimates of $g(\theta)$ were obtained for L1 and L2.

For this presentation, we also focus on measurements made by four stations with solar zenith angles differing significantly at the time of the SRB. The results are presented in Figure 5 for GPS SVID 15 L1 and L2 signals.

Figure 5a shows ΔC/No curves which are computed by subtracting the C/No curve of the previous days (without SRB) from the C/No curve observed on the day of the SRB, that is, $\Delta C/No = C/No^{Aug.\ 28} - C/No^{Aug.\ 27}$. ΔC/No curves are shown for receivers located in Presidente Prudente – Brazil (22.12°S,

51.41°W), Logan – US (41.93°N, 111.43°W), Colorado – US (38.38°N, 103.16°W), and Dallas – US (32.99°N, 96.75°W). The solar incidence (or zenith) angles for these stations at 18:00 UT are 49.1°, 37.6°, 31.3°, and 24.4°, respectively. The calculations took into consideration the variation of solar zenith angles with time. The results in Figure 5a show the solar zenith control over the magnitude of the fadings. It shows that as the local solar zenith angle decreases, the magnitude of the C/No fadings increases. For instance, at Presidente Prudente where the solar zenith angle is the largest during the SRB, the maximum C/No decrease was approximately 5 dB-Hz. In Dallas, however, where the solar zenith angle was the smallest, the maximum fading reached almost 8 dB-Hz.

Figure 5b shows the vertical equivalent ΔC/No curves calculated using equation (2). The results show an overall excellent agreement for the maximum C/No fadings estimated from different observations. It also shows a maximum fading depth of about 9 dB-Hz around 18:15 UT. Furthermore, it provides unequivocal evidence of the solar origin of the fadings.

Figure 5c provides results for analyses of the GPS SVID 15 L2 signal. Figure 5c shows ΔC/No for the L2 signal measured by the same four stations of Figure 5a. Again, the results confirm the overall solar zenith control of the observed fadings with larger depths in Dallas compared to Presidente Prudente, for instance. Figure 5d also shows the overall agreement between the zenith equivalent (maximum) fadings estimated from the four stations. While the maximum fading at L1 (~9 dB-Hz) occurred around 18:15 UT, the maximum fading for L2 occurred around 18:35 UT and reached approximately 13 dB-Hz. This can be interpreted as a result of the different temporal variations of the SRBs at different frequencies.

4 Summary and concluding remarks

We have deployed low-cost GNSS-based monitors of ionospheric scintillation and TEC over the American sector with the goal of studying low and mid-latitude ionospheric irregularities and scintillation. During a routine inspection of the observations made by a monitor located in Dallas, US, we observed unusual increases in the amplitude scintillation index (S_4) during daytime hours.

Inspection of observations made by other monitors of our network showed similar increases in S_4 during the same time. Additionally, TEC measurements also made by the monitors did not show evidence of ionospheric irregularities. The distributed, dual-frequency observations allowed us to rule out the possibility of L-band scintillation caused by daytime irregularities such as those associated with sporadic E-layers for instance (Seif et al., 2017). Instead, they led us to find that the S_4 increases resulted from C/No variations caused by a SRB event associated with two M-class X-ray solar flares and a Halo CME that occurred on 28 August 2022.

Further inspection of the observations allowed us to quantify the impact of the SRB. We showed that the SRB caused C/No fadings of up to ~8 dB-Hz on L1 (~1.6 GHz) signals and ~10 dB-Hz on L2 (~1.2 GHz) signals observed by the monitor in Dallas. Calculations using observations made by the distributed monitors also show good agreement for estimates of the maximum (vertical equivalent) C/No fadings. The calculations show maximum fadings of 9 dB-Hz for L1 and of 13 dB-Hz for L2.

The results exemplify the usefulness of the ScintPi monitors for studies beyond those associated with ionospheric irregularities and scintillation. The instrumentation can contribute with auxiliary observations of L-band RHCP SRBs and with investigations of the impact of SRBs on GNSS signals. For instance, the ScintPi array detected the 28 August 2022 SRB when the Owens Valley Solar Array (OVSA) was not making measurements. In addition to determining fading depths, the high sampling rate observations provided by the ScintPi monitors also allow one to quantify the effect of SRBs through the commonly used S_4 indices.

The S_4 values provided by the ScintPi monitors are examined routinely as part of our search for ionospheric scintillation events. Therefore, the S_4 indices can also help to detect SRBs as they occurred in the case of the SRB reported here. ScintPi monitors do not perform well in the region of small S_4 values (say $S_{4,L1} < \sim 0.2$) as mentioned by Gomez Socola & Rodrigues (2022) and, therefore, might not be as effective in detecting fadings caused by weak SRBs. A single station would be limited to observations during local daytime when the sun is above the low-gain portion of the antenna pattern, that is, above low-elevation angles. The low cost of the monitors, however, allows them to be deployed at different longitude sectors so that SRB effects can be observed at all universal times.

Acknowledgements. We would like to take the opportunity to thank John S. "Jack" Erickson from Schenectady, NY. Jack recently passed away on March 13, 2023, and was the first citizen scientist to volunteer to host one of our ScintPi 3.0 monitors. His willingness to help is much appreciated. Work at UTD was supported by the National Science Foundation (NSF) Award AGS-2122639 and by the NSF's GRFP Grant No. 2136516. Any opinions, findings, conclusions, or recommendations expressed in this material are those of the author(s) and do not necessarily reflect the views of the NSF. The Jicamarca Radio Observatory is a facility of the Instituto Geofisico del Peru operated with support from the NSF AGS-2213849 through Cornell University. JFGM would like to thank support to INCT through grants CNPq 465648/2014-2, CAPES (23038.000776/2017-54) and FAPESP (2017/50115-0). IP would like to thank support from the Conselho Nacional de Desenvolvimento Científico e Tecnológico (306063/2020-4) and Fundação de Amparo à Pesquisa do Estado da Paraíba (Demanda Universal). CGMB and PT would like to thank the support from NSF Award AGS-2221770. The editor thanks S. Tulasiram and an anonymous reviewer for their assistance in evaluating this paper.

Data availability

The ScintPi observations used in this study were placed in a public data repository (zenodo.org) at https://zenodo.org/records/10014974.

The GOES-17 satellite X-ray data used in this study was made available by the National Oceanic and Atmospheric Association (NOAA) at https://www.ngdc.noaa.gov/stp/satellite/goes-r.html. SRB reports were obtained from the Solar and

Geophysical Event report prepared by NOAA and made available through FTP (ftp://ftp.swpc.noaa.gov/pub/indices/events/). CME reports were obtained from the SOHO LASCO CME Catalog (https://cdaw.gsfc.nasa.gov/CME_list/). This CME catalog is generated and maintained at the CDAW Data Center by NASA and The Catholic University of America in cooperation with the Naval Research Laboratory. SOHO is a project of international cooperation between ESA and NASA.

References

Afraimovich EL, Demyanov VV, Ishin AB, Smolkov G Ya. 2008. Powerful solar radio bursts as a global and free tool for testing satellite broadband radio systems, including GPS–GLONASS–GALILEO. *J Atmos Sol Terr Phys* **70(15)**: 1985–1994. https://doi.org/10.1016/j.jastp.2008.09.008.

Afraimovich EL, Demyanov VV, Smolkov GY. 2009. The total failures of GPS functioning caused by the powerful solar radio burst on December 13, 2006. *Earth Planet Space* **61**: 637–641. https://doi.org/10.1186/BF03352940.

Bastian TS, Benz AO, Gary DE. 1998. Radio emission from solar flares. *Annu Rev Astron Astrophys* **36**: 131–188. https://doi.org/10.1146/annurev.astro.36.1.131.

Basu S, Basu S, Mullen JP, Bushby A. 1980. Long-term 1.5 GHz amplitude scintillation measurements at the magnetic equator. *Geophys Res Lett* **7**: 259–262. https://doi.org/10.1029/GL007i004p00259.

Carrano CS, Bridgwood CT, Groves KM. 2009. Impacts of the December 2006 solar radio bursts on the performance of GPS. *Radio Sci.* **44**: RS0A25. https://doi.org/10.1029/2008RS004071.

Claßen HT, Aurass H. 2002. On the association between type II radio bursts and CMEs. *A&A* **384(3)**: 1098–1106. https://doi.org/10.1051/0004-6361:20020092.

Correia E, Muella MTAH, Alfonsi L, Prol FS, Camargo PO. 2019. *GPS scintillations and total electron content climatology in the Southern American sector, accuracy of GNSS methods*. IntechOpen. https://doi.org/10.5772/intechopen.79218.

Cerruti AP, Kintner PM, Gary DE, Lanzerotti LJ, de Paula ER, Vo HB. 2006. Observed solar radio burst effects on GPS/Wide Area Augmentation System carrier-to-noise ratio. *Space Weather* **4**: S10006. https://doi.org/10.1029/2006SW000254.

Cerruti AP, Kintner PM Jr, Gary DE, Mannucci AJ, Meyer RF, Doherty P, Coster AJ. 2008. Effect of intense December 2006 solar radio bursts on GPS receivers. *Space Weather* **6**: S10D07. https://doi.org/10.1029/2007SW000375.

Chen Z, Gao Y, Liu Z. 2005. Evaluation of solar radio bursts' effect on GPS receiver signal tracking within International GPS Service network. *Radio Sci* **40**: RS3012. https://doi.org/10.1029/2004RS003066.

Coster AJ, Erickson PJ, Lanzerotti LJ, Zhang Y, Paxton LJ. 2021. *Space weather effects and applications. Geophysical Monograph Series*. American Geophysical Union. ISBN:9781119507574. https://doi.org/10.1002/9781119815570.

Demyanov VV, Afraimovich EL, Jin S. 2012. An evaluation of potential solar radio emission power threat on GPS and GLONASS performance. *GPS Solut* **16(4)**: 411–424. https://doi.org/10.1007/s10291-011-0241-9.

de Paula ER, Rodrigues FS, Iyer KN, Kantor IJ, Abdu MA, Kintner PM, Ledvina BM, Kil H. 2003. Equatorial anomaly effects on GPS scintillations in Brazil. *Adv Space Res* **31(3)**: 749–754. https://doi.org/10.1016/S0273-1177(03)00048-6.

de Paula ER, Martinon ARF, Carrano C, Moraes AO, Neri JACF, et al. 2022. Solar flare and radio burst effects on GNSS signals and the ionosphere during September 2017. *Radio Sci* **57**: e2021RS007418. https://doi.org/10.1029/2021RS007418.

Gomez Socola J, Rodrigues FS. 2022. ScintPi 2.0 and 3.0: low-cost GNSS-based monitors of ionospheric scintillation and total electron content. *Earth Planet Space* **74**: 185. https://doi.org/10.1186/s40623-022-01743-x.

Groves KM, Basu S, Weber EJ, Smitham M, Kuenzler H, et al. 1997. Equatorial scintillation and systems support. *Radio Sci* **32(5)**: 2047–2064. https://doi.org/10.1029/97RS00836.

Ishimaru A, Kuga Y, Liu J, Kim Y, Freeman A. 1999. Ionospheric effects on synthetic aperture radar at 100 MHz to 2 GHz. *Radio Sci* **34**: 257–268. https://doi.org/10.1029/1998RS900021.

Jiao Y, Morton YT. 2015. Comparison of the effect of high-latitude and equatorial ionospheric scintillation on GPS signals during the maximum of solar cycle 24. *Radio Sci* **50**: 886–903. https://doi.org/10.1002/2015RS005719.

Kelly MA, Comberiate JM, Miller ES, Paxton LJ. 2014. Progress toward forecasting of space weather effects on UHF SATCOM after Operation Anaconda. *Space Weather* **12**: 601–611. https://doi.org/10.1002/2014SW001081.

Kintner PM, Ledvina BM, de Paula ER. 2007. GPS and ionospheric scintillations. *Space Weather* **5**: S09003. https://doi.org/10.1029/2006SW000260.

Klobuchar J, Kunches J, VanDierendonck A. 1999. Eye on the ionosphere: potential solar radio burst effects on GPS signal to noise. *GPS Solut* **3**: 69–71. https://doi.org/10.1007/PL00012794.

Ledvina BM, Makela JJ, Kintner PM. 2002. First observations of intense GPS L1 amplitude scintillations at midlatitude. *Geophys Res Lett* **29(14)**: 4-1–4-4. https://doi.org/10.1029/2002GL014770.

Moraes AO, Rodrigues FS, Perrella WJ, de Paula ER. 2012. Analysis of the characteristics of low-latitude GPS amplitude scintillation measured during solar maximum conditions and implications for receiver performance. *Surv Geophys* **33(5)**: 1107–1113. https://doi.org/10.1007/s10712-011-9161-z.

Morosan DE, Kumari A, Kilpua EKJ, Hamini A. 2021. Moving solar radio bursts and their association with coronal mass ejections. *A&A* **647**: L12. https://doi.org/10.1023/A:1005075003370.

Mrak S, Semeter J, Nishimura Y, Rodrigues FS, Coster AJ, Groves K. 2020. Leveraging geodetic GPS receivers for ionospheric scintillation science. *Radio Sci* **55**: e2020RS007131. https://doi.org/10.1029/2020RS007131.

Muella MTAH, Kherani EA, de Paula ER, Cerruti AP, Kintner PM, Kantor IJ, Mitchell CN, Batista IS, Abdu MA. 2010. Scintillation-producing Fresnel-scale irregularities associated with the regions of steepest TEC gradients adjacent to the equatorial ionization anomaly. *J Geophys Res* **115**: A03301. https://doi.org/10.1029/2009JA014788.

Muhammad B, Alberti V, Marassi A, Cianca E, Messerotti M. 2015. Performance assessment of GPS receivers during the September 24, 2011 solar radio burst event. *J Space Weather Space Clim* **5**: A32. https://doi.org/10.1051/swsc/2015034.

Nita GM, Gary DE, Lee J. 2004. Statistical study of two years of solar flare radio spectra obtained with the Owens Valley Solar Array. *Astrophys J* **605**: 528–545. https://doi.org/10.1086/382219.

Rodrigues FS, Moraes AO. 2019. ScintPi: A low-cost, easy-to-build GPS ionospheric scintillation monitor for DASI studies of space weather, education, and citizen science initiatives. *Earth Space Sci* **6**: 1547–1560. https://doi.org/10.1029/2019EA000588.

Rodrigues FS, Socola JG, Moraes AO, Martinis C, Hickey DA. 2021. On the properties of and ionospheric conditions associated

with a mid-latitude scintillation event observed over southern United States. *Space Weather* **19**: e2021SW002744. https://doi.org/10.1029/2021SW002744.

Sato H, Jakowski N, Berdermann J, Jiricka K, Heßelbarth A, Banyś D, Wilken V. 2019. Solar radio burst events on 6 September 2017 and its impact on GNSS signal frequencies. *Space Weather* **17**: 816–826. https://doi.org/10.1029/2019SW002198.

Seif A, Liu J-Y, Mannucci AJ, Carter BA, Norman R, Caton RG, Tsunoda RT. 2017. A study of daytime L-band scintillation in association with sporadic E along the magnetic dip equator. *Radio Sci* **52**: 1570–1577. https://doi.org/10.1002/2017RS006393.

Sousasantos J, Gomez Socola J, Rodrigues FS, Eastes RW, Brum CGM, Terra P . 2023. Severe L-band scintillation over low-to-mid latitudes caused by an extreme equatorial plasma bubble: joint observations from ground-based monitors and GOLD. *Earth Planets Space* **75**: 41. https://doi.org/10.1186/s40623-023-01797-5.

Spogli L, Alfonsi L, Romano V, de Franceschi G, Monico G, Shimabukuro M, Bougar B, Aquino M. 2013. Assessing the GNSS scintillation climate over Brazil under increasing solar activity. *J Atmos Sol Terr Phys* **105**: 199–206. https://doi.org/10.1016/j.jastp.2013.10.003.

Sreeja V, Aquino M, de Jong K. 2013. Impact of the 24 September 2011 solar radio burst on the performance of GNSS receivers. *Space Weather* **11**: 306–312. https://doi.org/10.1002/swe.20057.

Sreeja V, Aquino M, de Jong K, Visser H. 2014. Effect of the 24 September 2011 solar radio burst on precise point positioning service. *Space Weather* **12**: 143–147. https://doi.org/10.1002/2013SW001011.

Valladares CE, Villalobos J, Sheehan R, Hagan MP. 2004. Latitudinal extension of low-latitude scintillations measured with a network of GPS receivers. *Ann Geophys* **22**: 3155–3175. https://doi.org/10.5194/angeo-22-3155-2004.

Yeh KC, Liu C-H. 1982. Radio wave scintillations in the ionosphere. *Proc IEEE* **70**: 324–360. https://doi.org/10.1109/PROC.1982.12313.

Yue X, Schreiner WS, Kuo Y-H, Zhao B, Wan W, et al. 2013. The effect of solar radio bursts on the GNSS radio occultation signals. *J Geophys Res Space Phys* **118**: 5906–5918. https://doi.org/10.1002/jgra.50525.

Yue X, Wan W, Yan L, Sun W, Hu L, Schreiner W. 2018. Chapter 22 - the effect of solar radio bursts on GNSS signals. In: *Extreme events Geospace orig. Predict. Cons*. Buzulukova N, (Ed.) Elsevier, Amsterdam. pp. 541–554. https://doi.org/10.1016/B978-0-12-812700-1.00022-4.

Cite this article as: Wright IG, Rodrigues FS, Gomez Socola J, Moraes AO, Monico JFG, et al. 2023. On the detection of a solar radio burst event that occurred on 28 August 2022 and its effect on GNSS signals as observed by ionospheric scintillation monitors distributed over the American sector. *J. Space Weather Space Clim*. **13**, 28. https://doi.org/10.1051/swsc/2023027.